Canadian Conference - Pacific Conference on Earthquake Engineering 2023
Vancouver, British Columbia
June 25th – June 30th, 2023

Assessment of Earthquake and Tsunami Risk for Tofino, British Columbia

Mark Novakovic[1], Jovana Borozan[1*], Karen Assatourians[1], Katsuichiro Goda[2], Karina Martinez- Alcala[2], Yusong Yang[2], Sheri Molnar[2], Hadi Ghofrani[2], Alex Bilson Darko[2], Alireza J. Samani[2], Natalia Gomez Jaramillo[2], Gail M. Atkinson[2], Tuna Onur[3] and Keith Orchiston[4]

[1]Nanometrics Inc, Kanata, ON, Canada
[2]Western University, London, ON, Canada
[3]Onur Seeman Consulting Inc, Victoria, BC, Canada
[4]District of Tofino, Tofino, BC, Canada
[*]jovanaborozan@nanometrics.ca (Corresponding Author)

ABSTRACT

A probabilistic earthquake and tsunami risk assessment was conducted for Tofino and neighboring Tla-o qui-aht First Nation (TFN) communities on Vancouver Island, British Columbia. It aims to provide guidance on disaster risk reduction planning at a local scale. The project is funded by the National Disaster Mitigation Program of Canada. The primary objective of the study is to estimate the hazard and potential loss due to earthquakes and tsunami in the region using a probabilistic analysis framework.

A probabilistic seismic hazard analysis (PSHA) was conducted to understand ground motion levels that can be produced by future earthquakes in the region. The 6th generation seismic hazard model of Canada ([1]) was adopted as a regional base model and was refined further in order to accurately represent the seismicity potential and resulting ground motions in the study area. The spatial variation of seismic site conditions and liquefaction susceptibility of soils were estimated using data acquired through a geotechnical assessment, which was conducted using non-invasive seismic field surveys across the study area. The subaqueous sources expose the coastal communities to tsunami risk as well. Probabilistic tsunami hazard analyses (PTHA) was conducted for near tsunamigenic sources using the conventional logic tree and more comprehensive stochastic approaches to generate hazard maps of various tsunami intensity metrics (e.g., maximum run-up, inundation depth and flow velocity) were generated. An exposure database of buildings and population was developed for risk assessment. Appropriate fragility and vulnerability models were combined with seismic and tsunami hazard estimates to determine the associated potential damage and loss.

The findings of the study will inform mitigation efforts, including the improvement of seismic resiliency in Tofino and TFN communities, design/assessment of tsunami vertical evacuation structures, development of evacuation routes and emergency response planning.

Keywords: seismic, hazard, risk, tsunami, loss

INTRODUCTION

The District of Tofino is located at the northern end of the Esowista Peninsula of Vancouver Island in British Columbia. It is situated within the Hahuulthii of the Tla-o-qui-aht Ha'wiih and is a hub of shared services for more than 4500 residents of West Coast communities living within the Clayoquot Sound Biosphere Region. To the west is the Pacific and the Cascadia Subduction Zone, which exposes Tofino and neighbouring communities to both earthquake and tsunami risk.

The tsunami risk to the region was explored at a high-level in a 2019 Comprehensive Coastal Flood Risk Assessment Project, funded by the National Disaster Mitigation Program. However, the study scope was limited in terms of tsunami risk assessment, using a deterministic (single-scenario) approach. Additionally, the previous functional studies that the District of

Tofino uses to prepare, respond, recover and mitigate risk did not evaluate the social and economic impacts of potential future earthquakes thoroughly. To better inform risk mitigation planning efforts, the District of Tofino (DoT) is interested in a comprehensive assessment of seismic and tsunami risk for the DoT and Tla-o-qui-aht First Nation (TFN) communities of Esowista, Ty-Histanis, and Opitsaht (hereafter referred to as the project area).

The primary objective of the study is to estimate the hazard as well as the associated damage and losses due to potential future earthquakes and tsunamis using a probabilistic analysis framework. The findings of this study will better inform the seismic and tsunami risk mitigation planning efforts, such as the improvement of seismic resiliency in DoT and TFN communities, design/assessment of Tsunami Vertical Evacuation (TVE) structures, development of evacuation routes and the planning of land use, infrastructure siting/design and emergency response. To this end, a geotechnical assessment is conducted in order to identify local site conditions and liquefaction susceptibility; an exposure model compiling information about buildings and populations in the region is developed; a seismic hazard assessment is performed to characterize ground motion levels that can be produced by future earthquakes; a seismic risk assessment is carried out to estimate the damages and losses associated with earthquakes in the region; and a tsunami hazard and risk assessment is conducted to assess the damages, losses and impacted areas for emergency response planning.

GEOTECHNICAL ASSESSMENT

A non-invasive seismic testing field campaign was conducted by a two-person field team within the District of Tofino including First Nation communities of Esowista and Tla-o-qui-aht, from November 19-23 2021. The obtained results were used to assess liquefaction susceptibility, average shear wave velocity in the upper 30m of a ground profile (referred to as V_{S30}, an indicator of ground stiffness) and site classification. Interpolated V_{S30} values mapped across the region are shown in Figure 1. Toward the north of Tofino and in Opitsaht we see typically higher V_{S30} values (indicating stiffer ground conditions) when compared to sites in southern Tofino and Esowista (indicating softer ground conditions or thick sediments). The resultant ground motions for northern Tofino and Opitsaht are expected to be relatively higher at short periods than sites in the south of Tofino and Esowista, where the opposite is true for long period motions. The liquefaction study showed areas with lower V_{S30} (<200 m/s) correlated with moderate liquefaction susceptibility where areas with intermediate (200 - 450 m/s) to high (> 450 m/s) V_{S30}'s correlated to low to very-low liquefaction susceptibility respectively.

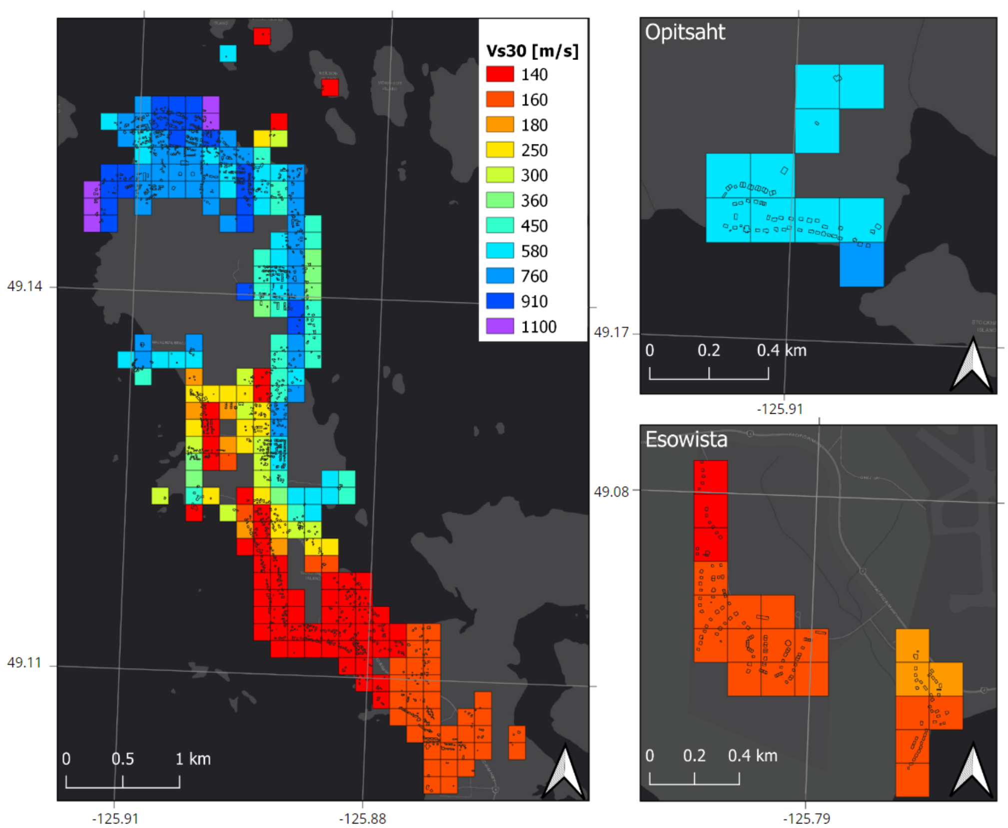

Figure 1. Map of interpolated V_{S30} values as determined in the geotechnical survey. Overlain in black are the building footprints from the exposure model.

SEISMIC HAZARD AND RISK ASSESSMENT

Probabilistic Seismic Hazard Assessment (PSHA)

Seismic hazard analyses in Western Canada are based on probabilistic concepts which allow incorporation of both geologic interpretations of seismic potential and statistical data regarding the locations and sizes of past earthquakes. The Cornell-McGuire method ([2], [3], [4], [5]) has proven particularly well-suited to calculate expected ground motions for a wide range of seismic hazard environments. It forms the basis for the seismic hazard maps in the National Building Code of Canada since 1985, and is the usual basis for seismic hazard evaluations of important engineered structures.

With probabilistic seismic hazard assessment (PSHA), ground motions that may be exceeded by future earthquakes at a target site can be estimated for a desired annual probability, considering uncertainties in their location, magnitude and ground motion. Uncertainties involved in PSHA are grouped into two categories: epistemic and aleatory uncertainty. The former refers to the model uncertainty due to incomplete knowledge regarding the processes governing earthquake occurrence and ground motion generation and is considered using a logic tree framework. The aleatory uncertainty, on the other hand, refers to the inherent random uncertainty due to the physical variability of earthquake rupture processes. It is incorporated directly into the probabilistic analysis as part of the integral sum of possible earthquake scenarios.

In this study, seismic hazard is determined based on the probabilistic method using the OpenQuake platform ([6], [7]). The spatial distribution of earthquakes is described by defining seismic source zones (areas which may contain groups of faults) on the basis of seismicity, linear fault sources and seismotectonic interpretations. The 6th generation source model of the GSC ([1]) is examined to determine whether it adequately represents the potential seismicity at the site vicinity and is considered as the base model for this study. The frequency of earthquake occurrence for each source zone is described by a magnitude-recurrence (MR) relationship, truncated at a maximum magnitude, Mmax.

An up-to-date earthquake catalog is compiled from public sources in order to validate the boundaries of seismic sources and their recurrence rates defined in the base model. It is found that the source zone definitions from the 6th generation hazard model adequately capture the important seismogenic sources on a regional level and the magnitude recurrence rates are not sensitive to the addition of more recent events. As such, the base model is adopted (Figure 2) as is and literature is reviewed to identify whether any additional local seismogenic sources should be considered in the source model to better reflect seismicity potential in the vicinity of the study area. The Beaufort Fault system was identified as a potential seismogenic source for consideration that could contribute to the hazard at the site. The Beaufort Fault is located roughly 70 km to the north east of the District of Tofino and was suggested to have been the host of the 1946 M7 earthquake and subsequent aftershock sequence. Limited information that can be linked to the activity rate of the fault is available. A recent paleoseismicity conference abstract [8] found that in the last ~13-11 kyr, approximately 7.5m of slip has occurred on the fault. Considering fault geometry scaling relationships ([9]), 7.5m of slip on the fault is the equivalent of four M7.5 events with an average return period on the order of ~2500 years. Sensitivity analysis is performed by adding the Beaufort fault to the seismic source model considering a return period of 1200 years for a M7.5 event to account for uncertainties. It is found that even with the conservative estimate of the earthquake return period, the fault makes no appreciable contribution to the hazard for all return periods due the proximity of the site to the Cascadia Subduction Zone, which is expected to dominate the hazard. The seismic potential of the Beaufort fault is considered to be implicitly captured by the Vancouver Island Coastal Range (VICM) source zone.

Earthquake ground-motion models (GMMs) provide the link between the occurrence of earthquakes of various magnitudes and the resulting ground motion levels at the site. Two suites of GMMs are considered in this hazard analysis. Active crustal sources are modeled by four of the GMMs developed for Western North America in the Next Generation Attenuation - West (PEER NGA-West2) ([10]) project. The epistemic uncertainty in median predictions is modeled based on a logic-tree approach. Al Atik & Youngs (2014) ([11]) suggest that considering the variability between the models alone may underestimate the epistemic uncertainty required to represent the potential range of alternative GMMs. The association of seismicity to specific faults or rupture orientations is not any better in active crustal sources in the vicinity of the project area than in other parts of Canada. To this end, rather than defining specific rupture parameters and generating ground motion tables a priori, pseudo-ruptures were generated in the OpenQuake platform by sampling a series of possible rupture parameters. Alternative strikes, dips and rakes are defined for areal active crustal sources with associated weights based on predominant faulting style within the source zone. This approach provides an additional measure of epistemic uncertainty in the analysis and is consistent with the degree of understanding of the earthquake rupture process as well as the GSC's approach in the 6th generation hazard model ([12]). Aleatory variability of ground motions is treated independently from the specification of the median ground motions and associated epistemic uncertainties. The authors provided recommended aleatory uncertainty models for use with each GMM and are considered in this study. For interface and inslab subduction sources, a subset of the recently developed NGA-Subduction ([13], [14], [15]) model suite is adopted with their associated uncertainties. Although the median amplitudes estimated by the updated ground motion model suite are broadly similar to the older suite used by the GSC, the associated aleatory uncertainties at shorter periods are appreciably greater.

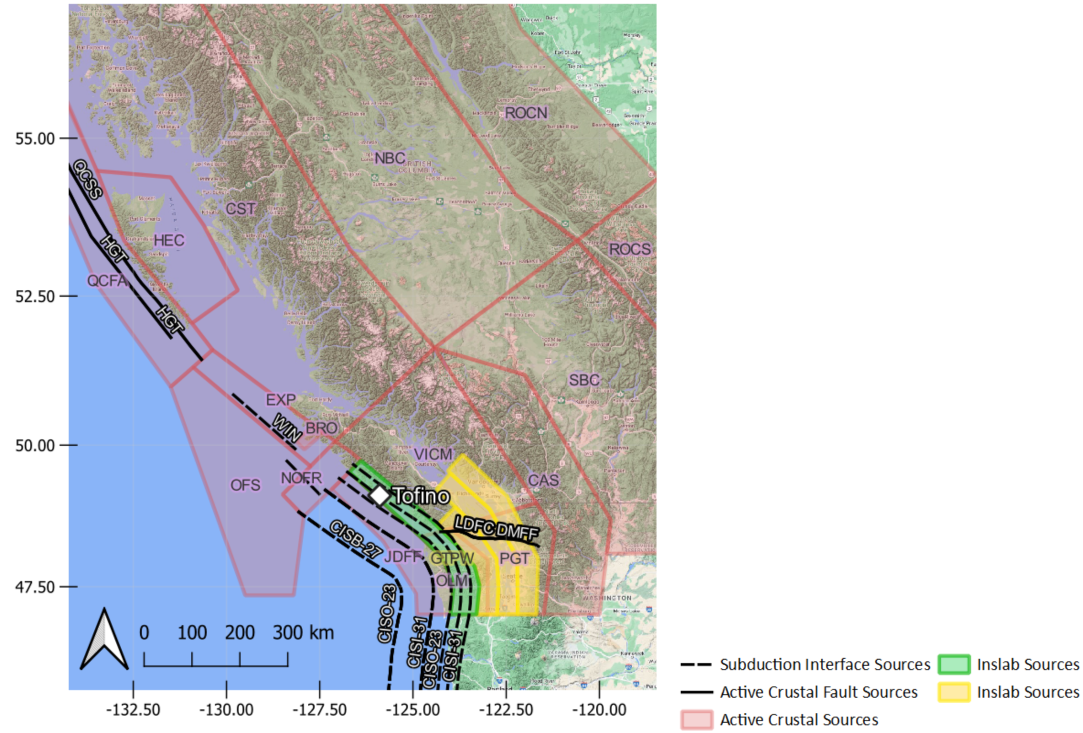

Figure 2. Base seismic source model, showing seismogenic sources surrounding Tofino. Subduction interface sources are shown as dashed lines, characterized active crustal faults are shown in solid lines, pink polygons show active crustal sources, green polygons show the relatively shallow Juan de Fuca inslab areal source and yellow show the relatively deeper inslab areal source zones for the Straight of Georgia (GTPW, GTPC and GTPE).

The probability of exceeding a specified level of ground motion at a site is calculated by summing up the hazard contributions over all magnitudes and distances. A Monte Carlo sampling approach is leveraged in this study in order to generate a synthetic ground motion catalog by sampling the seismic source model and ground motion model logic trees. The synthetic ground motion catalog generated during the hazard analysis is used as an input to the Seismic Risk Assessment.

In this study, hazard analysis is performed for 11 spectral periods of interest between 0.02 s $\leq$ T $\leq$ 10 s as well as for peak ground acceleration (PGA) to calculate UHS for each annual probability of interest (1/100, 1/475, 1/975 and 1/2475) for a suite of representative site conditions. Compared to the GSC's 6th generation hazard estimates, the hazard presented in this study is generally higher at short periods (T < 1s) and lower at intermediate to long periods (T > 1s) (Figure 3). The differences are primarily attributable to the increased aleatory uncertainties in the updated ground motion model suite used for estimating ground motions resulting from subduction earthquakes. The hazard maps indicate that in the northern end of Tofino and Opitsaht is characterized typically by stiffer sites, low hazard is expected at longer periods and relatively higher hazard at short periods whereas the opposite is true for sites further to the south. For Esowista, the area is characterized by generally low velocity sediments resulting in relatively higher hazard at long periods and relatively lower hazard at short periods. Figure 4 depicts a hazard map for PGA for a 2475 year return period.

The hazard is disaggregated to identify the dominant earthquake scenarios which contribute most to the hazard at the site. At the 100-year return period level, three main scenarios are present: crustal/inslab events with an average magnitude of 6.1 at rupture distances of approximately 60 km at short periods and events with M6.6-7 at distances of 110-150 km at long periods; a magnitude 7.9 event on the Explorer subduction interface at rupture distances of approximately 90 km across all ground motion parameters; and a Cascadia subduction interface event with a magnitude of 8.8 and rupture distance of 30 km for all ground motion parameters. In Figure 5, disaggregation plots of 1/100 and 1/2475 per annum (p.a.) PGA and spectral accelerations at 2.0s are shown. For the 475-, 975- and 2475-year return periods, the hazard is almost entirely dominated by Cascadia subduction interface events with magnitudes of 8.0- 8.8 at rupture distances of ~30 km.

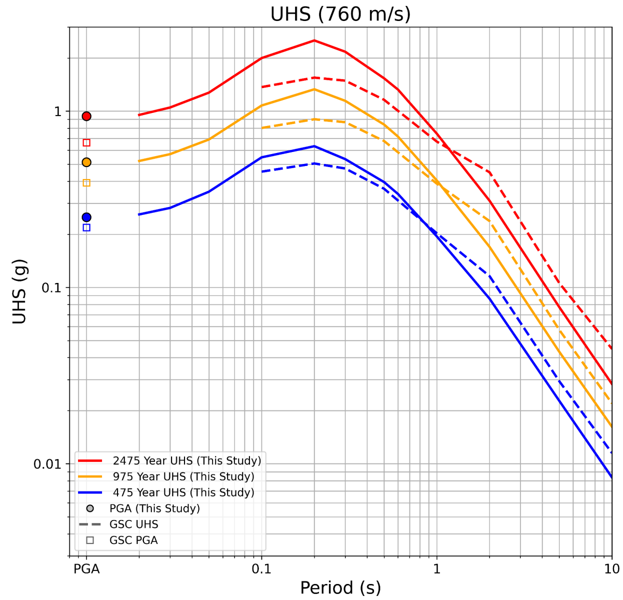

Figure 3. Comparison of horizontal-component UHSs for the B/C boundary site condition at Tofino (solid line) for the 475-, 975- and 2475-year return periods with the GSCs 6th generation UHS (dashed line, NBCC 2020 [16]).

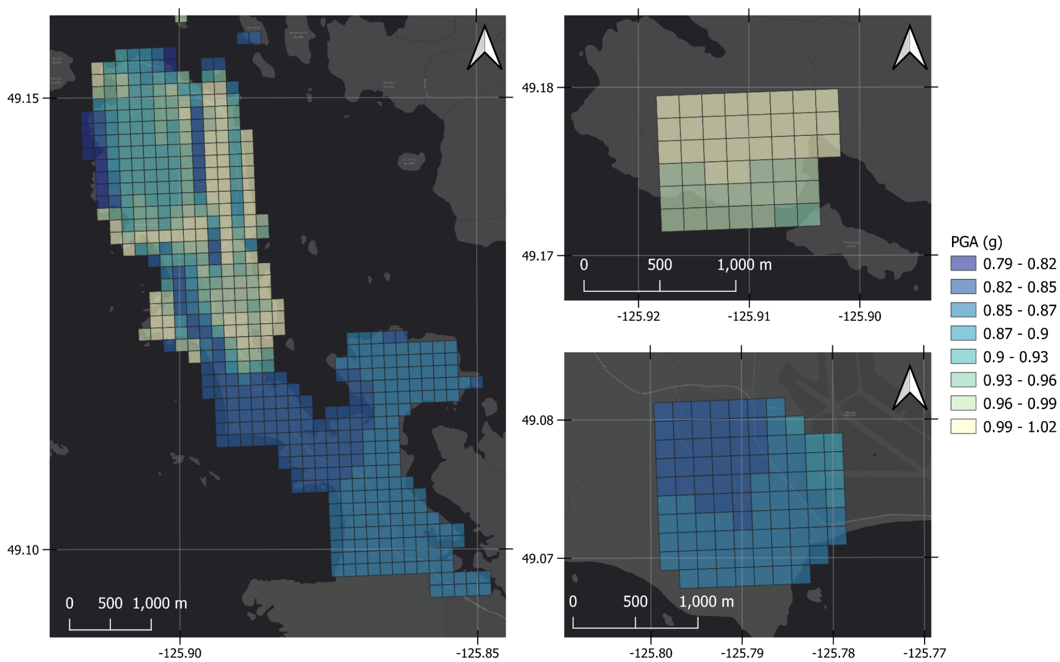

Figure 4. Hazard maps for the 2475-year horizontal-component PGA across Tofino (left), Opitsaht (upper right) and Esowista (lower right).

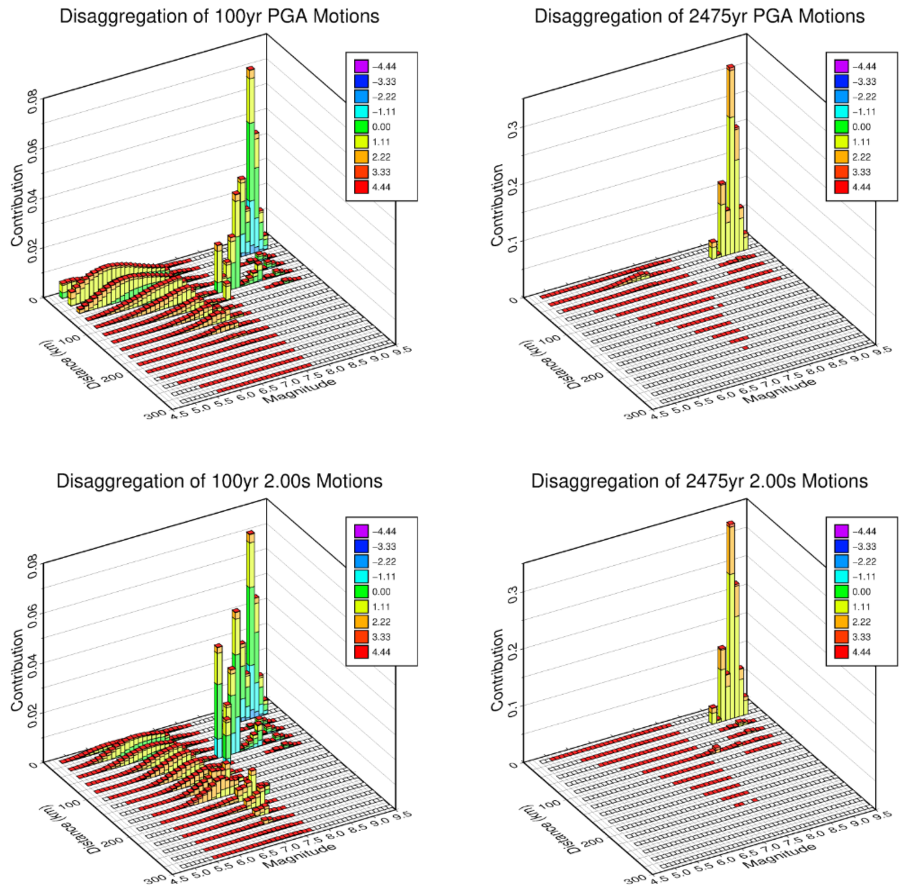

(a) *(b)*

Figure 5. Disaggregation for Tofino and neighboring TFN communities for (a) 100 year UHS and (b) 2475 year UHS. The bar size represents relative hazard contribution for each magnitude-distance pair. Colors indicate a breakdown of hazard contribution in terms of epsilon (ε), a measure of how far from the mean are the motions that are contributing to the overall hazard for a given magnitude-distance bin.

Probabilistic Seismic Risk Assessment (PSRA)

Probabilistic seismic risk assessment conducted for the project area incorporates hazard model, exposure model and vulnerability/fragility models. These models were combined for the final appraisal of expected induced damage as well as financial and occupants fatality losses in Tofino and TFN communities.

An exposure model containing detailed qualitative and quantitative descriptions of buildings and people exposed to seismic and tsunami risks was developed for the project area. The data sources used to compile the exposure model include primarily reports and georeferenced data provided by the DoT, exposure database from NRCan's Canadian Seismic Risk Model (CanSRM, [17]), 2021 Census Data ([18]) and other publicly available data. Each asset in the exposure model was assigned a taxonomy using HAZUS ([19]) building classification system, which is a unique identifier specifying building structural type, occupancy class and seismic design code level. The model specifies other characteristics of each of the exposed assets including building location, square footage, period of construction, building height, replacement costs for structural, nonstructural and contents building elements, number of occupants during day and night etc. By capturing a soft-story effect, which is a major structural irregularity, the exposure model was improved upon further which led to a novel approach in seismic risk assessment and making the resulting exposure database much more representative of Tofino's building stock. This high-resolution exposure model was used in the seismic risk as well as the tsunami risk assessments in this study, and can be adopted for use in future studies. The distribution of building occupancy classes depicted in Figure 6 shows that the majority of the buildings in the project area are residential. Most of them are wood structures (followed by manufactured, steel, concrete, unreinforced masonry and reinforced masonry buildings) associated with pre-code seismic design level. The exposure model contains a total of 1789 buildings and a total exposed value of 2.27 billion CAD. The structural, nonstructural and contents replacement costs contribute approximately 20%, 70% and 10% to the total replacement cost (i.e. total value of the exposed buildings) respectively. Tofino is a tourist destination with an estimated peak summer day time population of ~9600 people and summer night population of ~11,600 people.

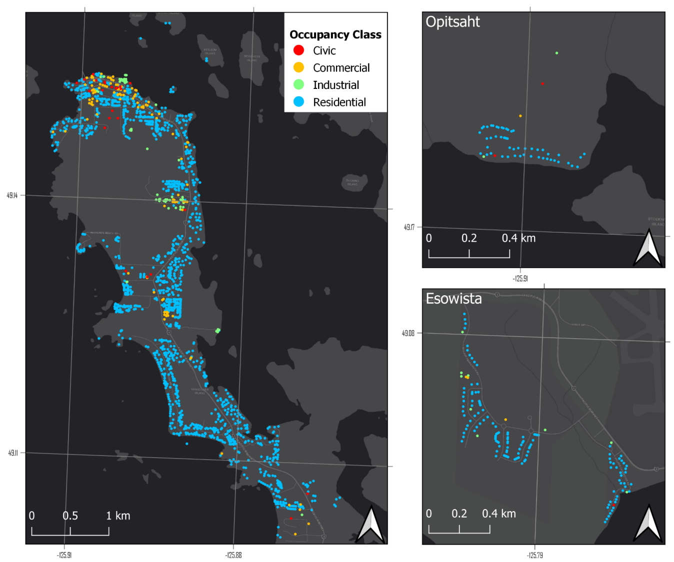

Figure 6. Distribution of building occupancy classes

Suitable fragility and vulnerability models were applied to assess performance of assets when subjected to differing levels of ground shaking. These models contain fragility/vulnerability curves for each of the building taxonomies specified in the exposure model. Fragility functions describe the likelihood that a building will experience different levels of damage with respect to a set of ground motion shaking intensity levels. They were used to assess the number of buildings in slight, moderate, extensive and complete damage states. Furthermore, the expected proportion of collapsed buildings was computed by combining structural fragility model with a consequence model specifying the ratio of collapses conditioned on a complete damage state. Vulnerability functions give a relationship between monetary and human losses with respect to a set of ground motion shaking intensity levels. They were used to assess the extent of the expected financial losses coming from structural, nonstructural and content building elements, as well as the number of the expected occupant fatalities. Fragility, vulnerability and consequence models were all adopted from NRCan ([20]; [17]).

The OpenQuake engine, developed by the Global Earthquake Foundation ([6], [7]), was used for probabilistic seismic risk assessment. The outputs are presented either as losses averaged on an annual basis or losses with respect to different return periods. The loss types covered by this project include financial loss (associated with structural, nonstructural elements and contents), occupants fatality loss and physical damage to buildings (slight, moderate, extensive, complete and collapse). Generated outputs include probabilistic loss maps, loss curves, average annual losses, as well as damage and collapse maps. The loss maps, loss curves and collapse maps were generated for four return periods of interest (100, 500, 1000 and 2475 years). The loss maps indicate that some assets may experience financial loss ratios as high as 60-80% for the return period of 2475 years (Figure 7). The financial loss ratio estimates become lower as return periods get smaller (up to 60% for 1000-, up to 40% for 500- and up to 20% for 100- year return period). For the return period of 2475 years, the total loss ratio (aggregated across all the assets) amounts to approximately 50% in terms of financial losses and 0.15% in terms of expected occupants' fatality losses (Figure 8). Expected average annual loss (AAL) is 0.1% ($2,304,910.50). The percentage contribution of structural, nonstructural and contents to the total financial AAL is 40%, 51% and 9% respectively. The estimated losses in terms of physical damage to buildings are on a lower side - which is due to the fact that only damage coming from structural elements was considered as well as the fact that although modifications to the assignment of design code levels were made in the exposure model to apply more conservative fragility models; the fragility curves used in damage estimation were developed without consideration of long-duration and high-intensity ground motions that are typical of the subduction zone in south-western British Columbia ([21]). Approximately 8 out of 1789 buildings present in the exposure model are expected to experience some level of damage on an annualized basis (mostly slight damage). The collapse ratio (expected proportion of collapsed buildings) for the return period of 100 years is negligible (lower than 0.1%) for most of the buildings, whereas for the return period of 2475 years some assets are expected to experience collapse ratios of up to 15% (Figure 9).

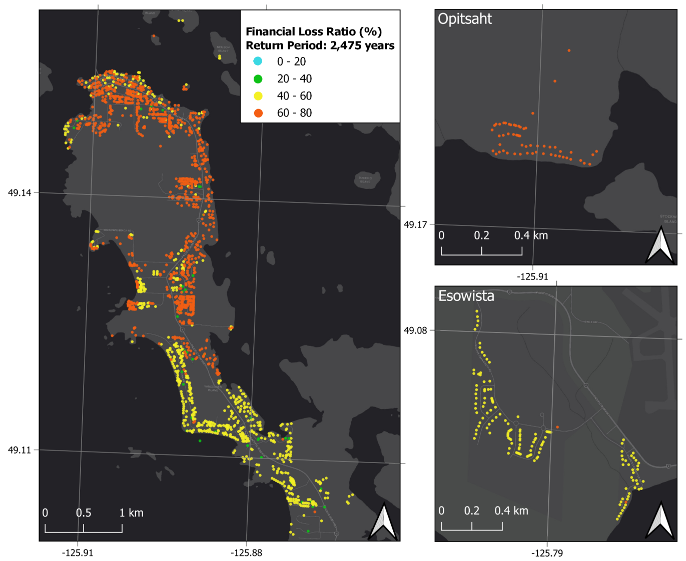

Figure 7. Financial loss ratio associated with 2475-years return period

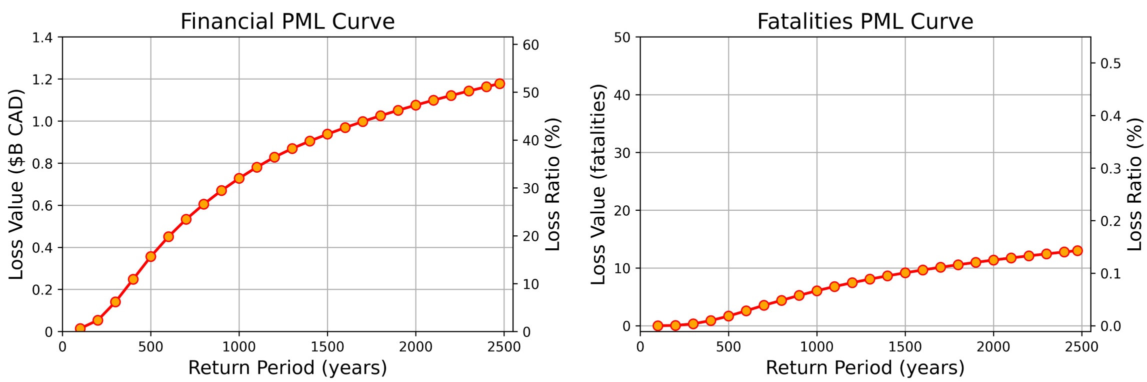

Figure 8. Probable Maximum Loss (PML) curves: (left) financial loss distribution, (right) fatality loss distribution.

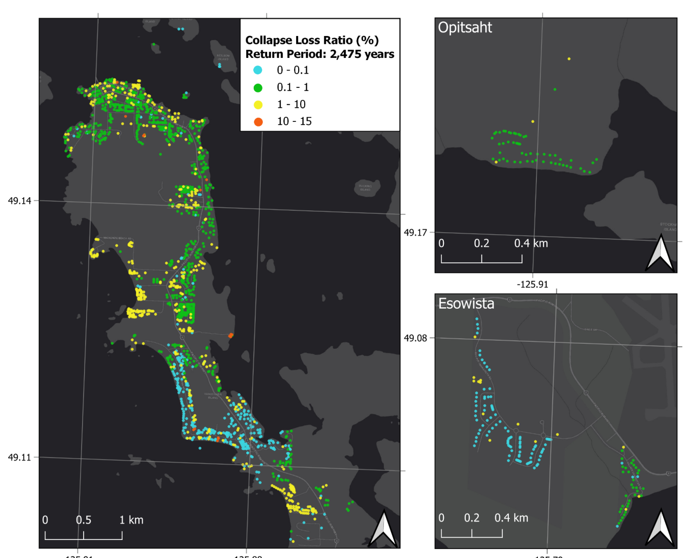

Figure 9. Collapse loss ratios associated with 2475-years return period.

PROBABILISTIC TSUNAMI HAZARD AND RISK ASSESSMENT

Background

Probabilistic tsunami hazard analysis (PTHA) and probabilistic tsunami risk analysis (PTRA) were performed for the DoT and the TFN communities. The probabilistic tsunami hazard model for the CSZ, which can host tsunamigenic megathrust events of Mw8.0+, is developed by incorporating the time-dependency of earthquake occurrence ([22]) and by adopting a stochastic source modeling approach ([23]). The PTHA elements can be decomposed into (i) time-dependent earthquake occurrence and rupture patterns, (ii) earthquake sources, and (iii) tsunami wave propagation and inundation. The final step (iv) involves the integration of the earthquake occurrence, sources, and tsunami simulation results to derive probabilistic tsunami hazard curves and maps. To conduct PTRA, exposure data and tsunami vulnerability functions need to be incorporated and combined with tsunami hazard estimates. Exposure data includes a database of exposed building assets and population. Tsunami fragility functions were developed using the extensive tsunami damage database from the 2011 Tohoku earthquake and tsunami ([24]). The fragility models can differentiate different building systems (masonry, wood, concrete, and steel) as well as topography (coastal plain versus ria). Finally, tsunami impact assessments were performed for critical infrastructures and facilities in the project area. The outputs were generated for 200, 500, 1000, 2500 and 5000 year return periods. They include site-specific tsunami hazard curves, tsunami hazard maps of different tsunami intensity metrics (e.g., maximum run-up, inundation depth, and flow velocity), as well as tsunami damage and loss maps encompassing the economic and social impacts.

Probabilistic Tsunami Hazard Assessment (PTHA)

To characterize uncertain earthquake occurrence from the CSZ, Holocene paleo-seismicity records ([25], [26]) are reviewed, and time-independent as well as time-dependent occurrence models are developed, which are associated with earthquake magnitude distributions and rupture patterns. This model component characterizes the earthquake occurrence frequency of the Cascadia events for different magnitudes and is the input into PTHA. For the time-dependent modeling, a renewal process is adopted in PTHA ([22]) such that the current elapsed time since the last major event in 1700 (i.e., 322 years) is reflected in the PTHA results.

To reflect realistic features of the earthquake rupture in terms of earthquake slip and fault geometry (as a function of earthquake magnitude), stochastic source models for the CSZ are developed ([27]). The stochastic method employs the statistical scaling relationships of earthquake source parameters and the stochastic earthquake slip synthesis ([28]). A full set of the stochastic sources (i.e., 500 models per 0.1-unit magnitude range; in total, 5000 stochastic models over the Mw8.1-Mw9.1 range) is used for the stochastic PTHA approach. The source models capture kinematic rupture processes with heterogeneous earthquake slip distributions. These features are critical in evaluating the tsunami hazard accurately; in comparison with conventional approaches of instantaneous rupture processes with uniform earthquake slip distributions, which tend to underestimate the tsunami hazard by a factor of 2 based on previous studies (e.g., [29]).

Once the earthquake source models are specified, water elevation changes due to the ruptures are calculated using [30] and [31] formulae and nonlinear shallow water equations are solved using the TUNAMI code ([32]). The outputs from the TUNAMI code include the water elevation and flow velocities (two horizontal directions), and therefore, can generate the necessary outputs for tsunami hazard and risk assessments (e.g., maximum inundation depth, flow velocity maps over an area as well as tsunami temporal profiles of water level and flow velocities at specific locations). The effects of the tidal levels can also be included by running tsunami simulations for different tidal conditions. Through the Monte Carlo tsunami simulations and probabilistic calculus, the results from the above-mentioned three components can be combined to produce the site-specific tsunami hazard curves at different return periods and the corresponding probabilistic tsunami hazard maps of tsunami intensity metrics (e.g., inundation depth and flow velocity). The detailed procedures can be found in [28] and [22].

A subset of the results are presented here. Figure 10 depicts tsunami planning maps for the tidal levels of 0m and 3m for the 500- and 2475-year return periods respectively to demonstrate the lower and upper ranges of results in the analysis. The hazard vulnerability classification maps were calculated and plotted to evaluate the potential consequences based on the composite tsunami hazard parameter D (water depth) ×V (flow velocity). By using the tsunami hazard quantities that are determined for different critical return period scenarios and tidal conditions, hazard vulnerability classification maps for the District of Tofino are evaluated for different tidal levels. Hazard vulnerability classification map for tidal levels 0m and 3m for the 500- and 2475-year return periods respectively are shown in Figure 11. Compared to the tsunami planning maps, the hazard vulnerability classification maps for Tofino show smaller areas that will be affected by tsunamis (primarily along the shorelines facing the Pacific).

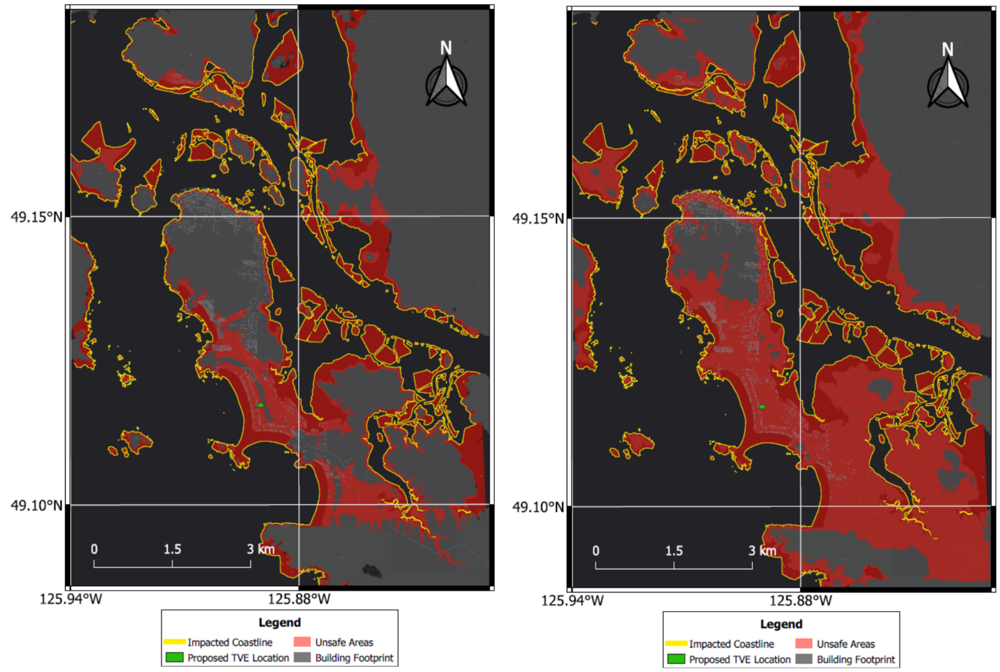

Figure 10. Tsunami planning maps, where the left panel depicts the 500 year return period level and a tidal level of 0m and the right shows the 2500 year return period level for a tidal level of 3m. Areas shaded in red indicate unsafe areas, light grey outlines depict building footprints and the green box to the south of the peninsula shows the proposed location of a Tsunami Vertical Evacuation (TVE) structure.

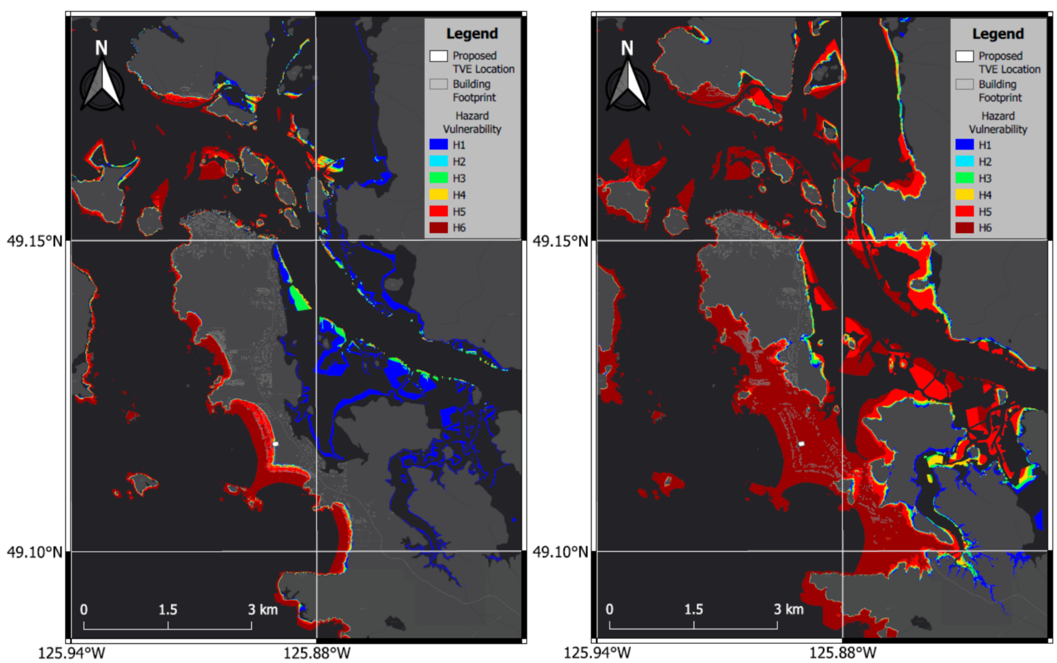

Figure 11. Tsunami hazard vulnerability classification maps, where the left panel depicts the 500 year return period level and a tidal level of 0m and the right shows the 2500 year return period level for a tidal level of 3m. H1 – generally safe for people, vehicles and buildings; H2 – unsafe for small vehicles; H3 – unsafe for vehicles, children, and the elderly, H4 – unsafe for people and vehicles; H5 – unsafe for vehicles and people, all buildings vulnerable to structural damage, some less robust building types vulnerable to failure; H6 – unsafe for vehicles and people, all building types considered vulnerable to failure.

CONCLUSIONS

Probabilistic seismic and tsunami hazard and risk analyses were carried out for the District of Tofino and the First Nations communities of Esowista, Ty-Histanis, and Opitsaht. The geotechnical field survey was conducted using non-invasive testing at multiple locations across the project area. The results were used to derive and map site conditions, V_{S30} values and liquefaction susceptibility. Higher V_{S30} values, observed in the northern part of Tofino and Opitsaht, indicate stiffer ground conditions when compared to the southern Tofino and Esowista associated with lower V_{S30} values.

The uniform seismic hazard spectra (UHS) was determined for four return periods of interest: 100, 475, 975, and 2475 years for 11 representative VS30 values. Hazard maps were generated for the project area, for each intensity parameter and return period. Disaggregation seismic hazard analyses indicate that the hazard is mostly controlled by large magnitude earthquakes at short distances (less than 40 km) for 2475-year, 975-year, and 475-year return periods level motions. These earthquakes correspond to Cascadia interface and include 80%-97% of contributions. However, there are three main scenarios contributing hazard at 100-year return period level, which are associated with inslab/shallow crustal, Explorer microplate and Cascadia interface sources.

A detailed database of exposed assets was developed under the scope of this project. It contains information related to buildings and occupants that are being exposed to the seismic and tsunami hazards in the project area. For each building in the exposed area, the exposure database defines structural type, occupancy class, building height, period of construction, seismic design levels, square footage as well as associated replacement costs and number of occupants. In addition, a soft-story structural irregularity was captured in the exposure model and this information was used in seismic risk analyses.

Probabilistic seismic damage and risk analyses were carried out using the OpenQuake engine by combining hazard model, fragility and vulnerability curves and the exposure model. Probabilistic loss maps describing expected financial loss, occupants fatalities and building collapses were developed for return periods of 100, 500, 1000 and 2475 years. Average annual loss and Probable Maximum Loss (PML) curves were also derived. The expected average annual loss amounts to 0.1% (~$2.3 million). The total loss ratio associated with the return period of 2475 years amounts to approximately 50% in terms of financial losses and 0.15% in terms of expected occupants' fatality losses.

The tsunami hazard and risk analyses indicates that the tsunami hazards and risks for the District of Tofino and the TFN communities are severe and when large earthquakes occur off Vancouver Island, extensive tsunami inundation will be caused, and numerous people and buildings will be affected by the tsunamis. Under these severe scenarios, critical infrastructures, such as roads and power lines, will also be significantly impacted. Although average tsunami risks are not particularly large, tail risks of the tsunami threats to Tofino are significant and potentially result in economic losses exceeding 500 billion CAD in Tofino alone. It is imperative to manage such low-frequency high-consequence risks effectively; otherwise, the future Cascadia subduction events will cause catastrophic long-term impacts to the communities in Tofino.

ACKNOWLEDGMENTS

We thank members of NRCan's Risk team, Tiegan Hobb and Philip LeSueur, for their guidance and contribution to this project, and for sharing the NRCan's exposure, fragility and vulnerability models that were used in this study.

REFERENCES

[1] Adams, J., T. Allen, S. Halchuk, and M. Kolaj (2019). Canada's 6th generation seismic hazard model, as prepared for the 2020 National Building Code of Canada. *12th Canadian Conference on Earthquake Engineering*, June 17 - 20, 2019, Quebec City, Quebec.
[2] Cornell, C.A. (1968). Engineering seismic risk analysis. *Bulletin of the Seismological Society of America*, 58: 1583-1606.
[3] McGuire, R. K. (1976). FORTRAN computer program for seismic risk analysis. *United States Geological Survey*.
[4] McGuire, R. K. (1977). Seismic design spectra and mapping procedures using hazard analysis based directly on oscillator response. *Earthquake Engineering and Structural Dynamics*, 5(3): 211 – 234.
[5] McGuire, R. K. (2004). Seismic hazard and risk analysis, EERI Monograph MNO-10. *Earthquake Engineering Research Institute*, Oakland, California.
[6] GEM (2022). The OpenQuake-engine User Manual. Global Earthquake Model (GEM) OpenQuake Manual for Engine version 3.15.0. doi: 10.13117/GEM.OPENQUAKE.MAN.ENGINE. 3.15.0
[7] Pagani, M., D. Monelli, G. Weatherill, L. Danciu, H. Crowley, V. Silva, P. Henshaw, L. Butler, M. Nastasi, L. Panzeri, M. Simionato, and D. Vigano (2014). OpenQuake engine: An open hazard (and risk) software for the global earthquake model. *Seismological Research Letters*, 85(3): 692-702.
[8] Lynch, E. M., C. Regalla, S. E. Bennett, K. D. Morell, L. J. Leonard, N. Harrichhausen, and E. Nissen (2022). Holocene Paleoseismicity in the northern Cascadia forearc: Non-steady slip on the right-lateral oblique Beaufort Range fault, Vancouver Island, Canada. *AGU Fall Meeting 2022*, Chicago, Illinois, December 11 - 15, 2022.

[9] Youngs, R. R. and K. J. Coppersmith (1985). Implications of fault slip rates and earthquake recurrence models to probabilistic seismic hazard estimates. *Bulletin of the Seismological Society of America*, 74(4): 939-964

[10] Bozorgnia, Y., L. Al Atik, G. M. Atkinson, A. Baltay, K. W. Campbell, R. Darragh, J. Donahue, N. Gregor, R. Kamai, A. Kottke, B. Rowshandel, T. Shantz, J. P. Stewart, and K. Wooddell (2014). NGA-West2 Research Project. *Earthquake Spectra*, 30(3): 973–987.

[11] Al Atik, L., and R. R. Youngs (2014). Epistemic uncertainty for NGA-West2 models. *Earthquake Spectra*, 30: 1301–1318.

[12] Kolaj, M., T. Allen, R. Mayfield, J. Adams, and S. Halchuk (2019). Ground-motion models for the 6th Generation seismic hazard model of Canada, *12th Canadian Conference on Earthquake Engineering*, June 17 - 20, 2019, Quebec City, Quebec, 192-hHtH-159.

[13] Abrahamson, N., N. Kuehn, Z. Gulerce, N. Gregor, Y. Bozognia, G. Parker, J. Stewart, B. Chiou, I. M. Idriss, K. Campbell, and R. Youngs (2018). Update of the BC Hydro subduction ground-motion model using the NGA-Subduction dataset. *Pacific Earthquake Engineering Research Center (PEER) Report* 2018/02.

[14] Parker, G., J. P. Stewart, D. M. Boore, G. M. Atkinson, and B. Hassani (2020). NGA-Subduction global ground-motion models with regional adjustment factors. *Pacific Earthquake Engineering Research Center (PEER) Report* 2020/03.

[15] Kuehn, N., Y. Bozorgnia, K. W. Campbell, and N. Gregor (2020). Partially non-ergodic ground-motion model for subduction regions using the NGA-Subduction database. *Pacific Earthquake Engineering Research Center (PEER) Report* 2020/04.

[16] National Building Code of Canada (NBCC, 2020). National Building Code of Canada 2020 Volume 1.

[17] Hobbs, T. E., J. M. Journeay, A. S. Rao, M. Kolaj, L. Martins, M. Simionato, V. Silva, M. Pagani, K. Johnson, D. Rotheram, and P. LeSueur (2022). The first public national Canadian seismic risk model: Scientific underpinnings and preliminary results for the pre-release. *12th National Conference on Earthquake Engineering*, Salt Lake City, Utah, June 27 - July 1, 2022.

[18] Statistics Canada (2021). Census Profile 98-316-X2021001. 2021 Statistics Canada Data Products,

[19] FEMA (2012). Multi-hazard loss estimation methodology earthquake model HAZUS-MH 2.1 technical manual. Department of Homeland Security Federal Emergency Management Agency Mitigation Division, Washington, D. C.

[20] Hobbs, T. E., J. M. Journeay, and D. Rotheram (2021). An earthquake scenario catalogue for Canada: A guide to using scenario hazard and risk results. *Geological Survey of Canada*, Open File 8806, 22 pp.

[21] Abraham, A., A. Bebamzadeh, and C. E. Ventura (2019). Seismic vulnerability in Southwestern BC - Impact of long duration subduction ground motion on wood typologies. *12th Canadian Conference on Earthquake Engineering*, Quebec City, Quebec, June 17 - 20, 2019.

[22] Goda, K. (2019). Time-dependent probabilistic tsunami hazard analysis using stochastic source models. *Stochastic Environmental Research and Risk Assessment*, 33: 341–358.

[23] Goda, K., T. Yasuda, N. Mori, and T. Maruyama (2016). New scaling relationships of earth-quake source parameters for stochastic tsunami simulation. *Coastal Engineering Journal*, 58(3): 1650010-1 - 1650010-40.

[24] De Risi, R., K. Goda, T. Yasuda, and N. Mori (2017). Is flow velocity important in tsunami empirical fragility modeling? *Earth-Science Review*, 166: 64–82.

[25] Goldfinger, C., C. H. Nelson, A. E. Morey, J. E Johnson, J. R. Patton, E. Karabanov, J. Gutiérrez-Pastor, A. T. Eriksson, E. Gràcia, G. Dunhill, R. J. Enkin, A. Dallimore, and T. Vallier (2012). Turbidite event history—Methods and implications for Holocene paleoseismicity of the Cascadia Subduction Zone. *USGS Professional Paper* 1661-F.

[26] Walton, M., L. Staisch, T. Dura, J. Pearl, B. Sherrod, J. Gomberg, S. Engelhart, A. Tréhu, J. Watt, J. Perkins, R. Witter, N. Bartlow, C. Goldfinger, H. Kelsey, A. Morey, V. Sahakian, H. Tobin, K. Wang, R. Wells, and E. Wirth (2021). Toward an integrative geological and geophysical view of Cascadia Subduction zone earthquakes. Annual Review of Earth and Planetary Sciences, 49: 367–398.

[27] Goda, K. (2022). Stochastic source modelling and tsunami simulations of Cascadia subduction earthquakes for Canadian Pacific coast. *Coastal Engineering Journal*, 64(4): 575-596.

[28] De Risi, R., and K. Goda (2017). Simulation-based probabilistic tsunami hazard analysis: empirical and robust hazard predictions. *Pure and Applied Geophysics*, 174: 3083–3106.

[29] Melgar, D., A. L. Williamson, and E. F. Salazar-Monroy (2019). Differences between heterogenous and homogenous slip in regional tsunami hazards modelling. *Geophysical Journal International*, 219: 553–562.

[30] Okada, Y. (1985). Surface deformation due to shear and tensile faults in a half-space. *Bulletin of the Seismological Society of America*, 75: 1135–1154.

[31] Tanioka, Y., and K. Satake (1996). Tsunami generation by horizontal displacement of ocean bottom. *Geophysical Research Letters*, 23: 861–864.

[32] Goto, C., Y. Ogawa, N. Shuto, and F. Imamura (1997). Numerical method of tsunami simulation with the leap-frog scheme. IOC Manual, UNESCO, No. 35, Paris, France.